
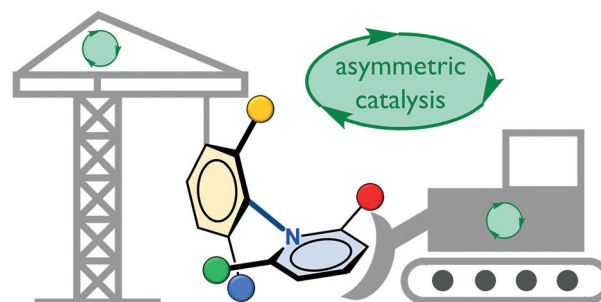


Catalytic Enantioselective Synthesis of C–N Atropisomeric Heterobiaryls

Jamie S. Sweet
Peter C. Knipe* 

School of Chemistry and Chemical Engineering, Queen's University Belfast, David Keir Building, Belfast, BT9 5AG, UK
p.knipe@qub.ac.uk



Received: 13.12.2021
Accepted after revision: 21.12.2021
Published online: 23.02.2022
DOI: 10.1055/s-0040-1719896; Art ID: ss-2021-r0762-sr

Abstract Molecules containing an atropisomeric C–N biaryl axis are gaining increasing attention in catalytic and medicinal chemistry. Despite this rising interest, relatively few approaches towards their catalytic enantioselective synthesis have been reported. Here we review these approaches, with a focus on the mechanism of asymmetric induction. Some common themes emerge: Brønsted acid catalysed cyclo-condensation and palladium-catalysed ring-closure are the most common and successful approaches. Meanwhile, the more direct but challenging axial C–N bond formation strategy remains in its infancy, with just two reports to-date. We hope this review will inform and inspire other researchers to develop new creative approaches to this important chemical motif.

- 1 Introduction
- 2 Cyclo-Condensation
- 3 Proximal C–N Bond Formation
- 4 Desymmetrisation of Intact Axes
- 5 *ortho*-C–H Functionalisation
- 6 Cycloaddition
- 7 Axial C–N Bond Formation
- 8 Atropisomeric N–N Axes: An Emerging Class of Heterobiaryls
- 9 Conclusion and Outlook

Key words enantioselectivity, atropisomerism, asymmetric catalysis, axial chirality, heterocycles, heterobiaryls

1 Introduction

Isomerism arising from restricted rotation about a single bond, atropisomerism, was first proposed by Christie and Kenner for hindered 2,2',6,6'-tetrasubstituted biphenyl derivatives in 1922.¹ In 1931, the first example of a C–N heterobiaryl atropisomer was reported by Adams and Bock.² In the years since, C–C atropisomers have become central to synthetic organic chemistry, in particular due to

the ubiquity of the 1,1'-binaphthyl motif at the core of numerous chiral ligands and organocatalysts. By contrast, C–N atropisomerism has remained relatively overlooked. However, the importance of these molecules is increasingly emerging across chemistry and biology. New organocatalysts³ and ligands for metal-catalysed cross-coupling containing C–N chiral axes have recently been reported,^{3b,4} hinting at the general utility of such molecules for asymmetric catalysis applications (Figure 1). The medical importance of C–N atropisomers⁵ was recently highlighted by the FDA approval of Amgen's first-in-class KRAS inhibitor Sotorasib,⁶ which contains an atropisomeric *N*-arylquinazolin-2-one linkage.



Peter C. Knipe received his M.Sc. in 2008 from the University of Cambridge. He then moved to the University of Oxford to undertake a Ph.D. under the tutelage of Martin D. Smith, examining counterion control in enantioselective electrocyclic reactions. Following this, he joined the laboratory of Andrew D. Hamilton as a postdoctoral researcher, where he focused on the applications of artificial macromolecules as potential therapeutics targeting protein-protein interactions. In 2016 he joined Queen's University Belfast as a lecturer in organic chemistry. His current research interests span asymmetric catalysis, synthetic organic, continuous flow, supramolecular and macromolecular chemistry, and their applications in the synthesis of bioactive compounds of therapeutic relevance.

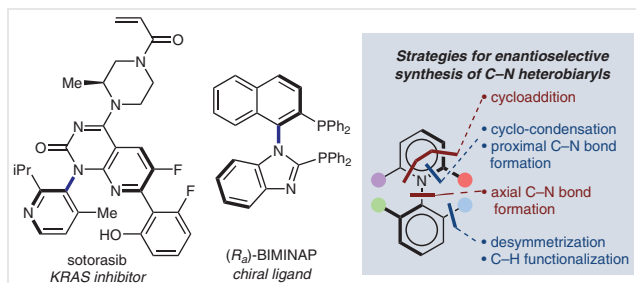


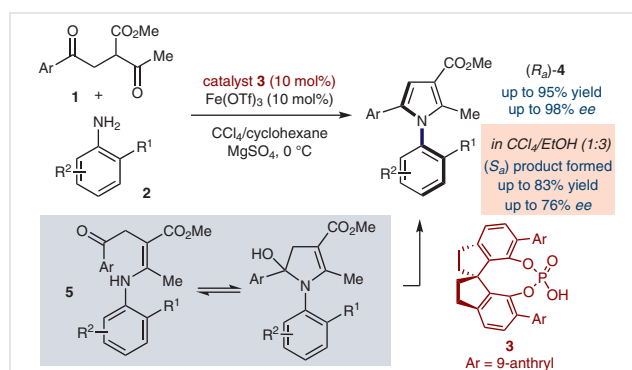
Figure 1 Left: medicinally and catalytically important C-N heterobiaryls. Right: schematic overview of strategies towards C-N heterobiaryls discussed in this review.

The heteroaromatic structure lends itself to many synthetic strategies not accessible to homobiaryl C-C atropisomers, such as metal-catalysed C-N bond formation and organocatalytic condensation reactions. Since 2008 there has been an explosion in catalytic enantioselective approaches towards C-N heterobiaryl atropisomers. This review attempts to summarise and categorise these developments, with reactions grouped by the strategic bond-forming approach taken to control axial stereochemistry. We have drawn particular attention to substrate-catalyst interactions (where such details have been provided by authors), in the hope that the reader may gain a greater understanding of the origins of enantiocontrol in the formation of C-N heterobiaryl atropisomers, and be inspired to make new creative developments in this field. Readers are encouraged to consult the primary texts for further details of all mechanistic and stereochemical proposals provided and the evidence underpinning them. This review does not seek to discuss the numerous elegant approaches to *non*-heterobiaryl C-N atropisomers (where one or both termini of the axial C-N bond are not aromatic rings) and readers are referred to several excellent reviews for discussion of those aspects.⁷

2 Cyclo-Condensation

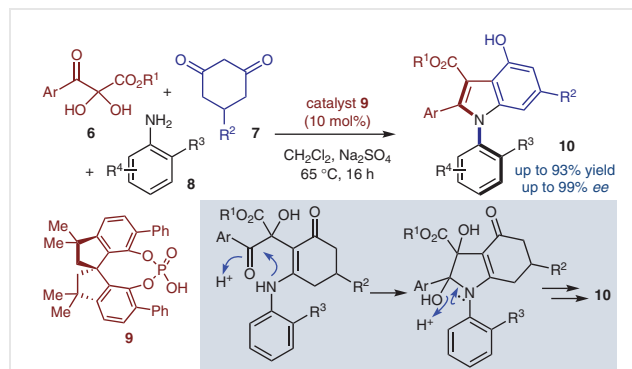
The classical approach to aza-heterocycle synthesis is through condensation chemistry (e.g. Paal-Knorr, Friedlander, Skraup, etc.) and the majority of these processes are acid catalysed. It is unsurprising therefore, with the advent of powerful chiral acidic organocatalysts, that this condensation approach has been brought to bear on the challenge of enantioselective synthesis of C-N atropisomers. The group of Bin Tan has been prolific in the use of chiral phosphoric acids (CPAs) for the enantioselective synthesis of heterobiaryls.^{7h} In 2017, the Tan group employed CPA catalysis when synthesising *N*-arylpyrroles via an enantioselective Paal-Knorr reaction (Scheme 1).⁸ 1,4-Diketones **1** and 2-substituted anilines **2** successfully underwent dehydrative cyclisation in the presence of SPINOL-derived CPA **3** and Fe(OTf)₃ in CCl₄/cyclohexane at 0 °C. They reported ex-

cellent yields (up to 95%) and enantioselectivities (up to 98% ee) for a range of axially chiral *N*-arylpyrroles **4**. An interesting solvent effect was observed in which the opposite *N*-arylpyrrole enantiomer could be obtained, albeit at lower ee values, by changing one solvent from the mixture of cyclohexane and non-polar CCl₄ [96% ee, (*R*_a)-**4**] to cyclohexane and polar protic EtOH [–75% ee, (*S*_a)-**4**], though the reasons for this stereodivergence are not further expounded. The isolation of intermediate **5** led the authors to propose the mechanism given, though it is not stated whether the reaction proceeds through centre-to-axis chirality transfer from the chiral hemi-aminal, or by atroposelective elimination of water.



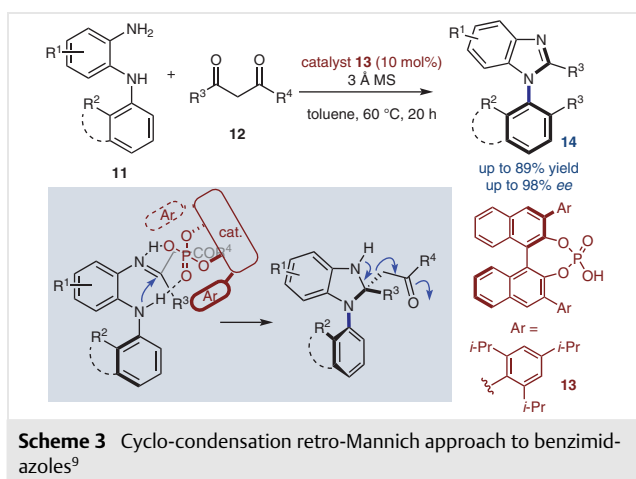
Scheme 1 Phosphoric acid catalysed cyclocondensation approach to *N*-arylpyrroles⁸

Lin and co-workers reported the synthesis of axially chiral *N*-arylindoles through a three-component coupling approach (Scheme 2).^{4b} When *ortho*-substituted anilines **8**, 2,3-diketone ester hydrates **6**, and cyclohexane-1,3-diones **7** were combined in the presence of a SPINOL-type chiral phosphoric acid **9**, chiral indole products **10** were obtained in up to 93% yield and 99% ee. The authors' mechanistic proposal closely resembles that of Tan (Scheme 1), though specific substrate-catalyst interactions leading to the observed atropisomer are not discussed.

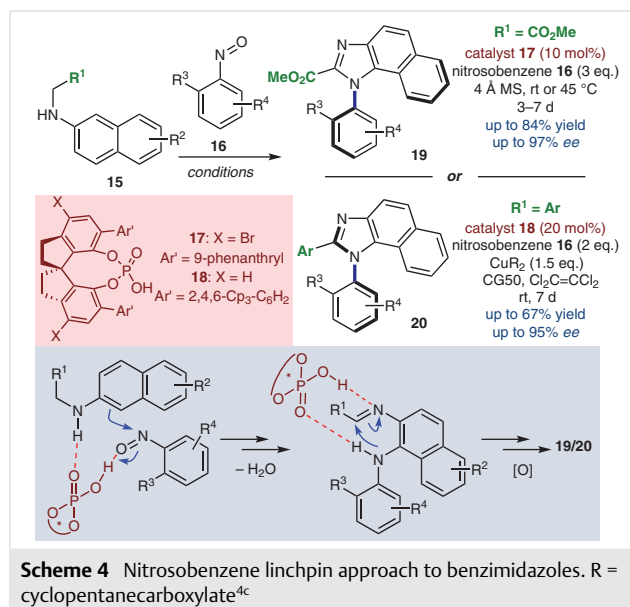


Scheme 2 CPA-catalysed three-component synthesis of *N*-arylindoles^{4b}

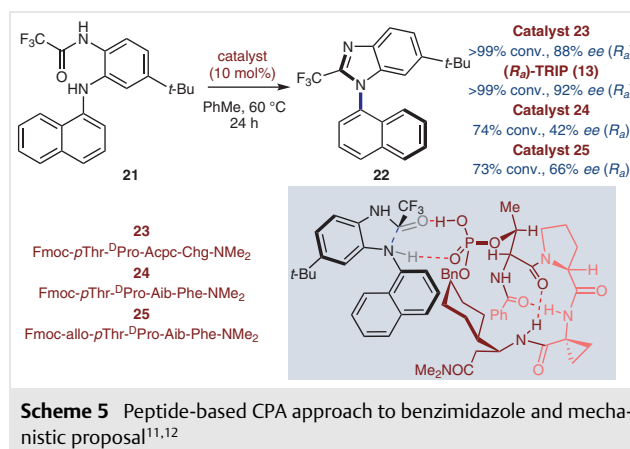
More recently in 2020, benzimidazoles have been synthesised via acid-catalysed cyclo-condensation (Scheme 3). Fu and co-workers synthesised axially chiral C–N atropisomeric benzimidazoles **14** in excellent enantioselectivity (up to 98% ee) and in high yields (up to 89%) from *N*-aryl-phenylenediamines **11** and 1,3-diketones or β -keto esters **12** in the presence of CPA (R_a)-TRIP **13**.⁹ The reaction is suggested to proceed via CPA-controlled aminal formation, followed by a retro-Mannich reaction to form the benzimidazole, similar to that previously reported by Tan¹⁰ (Scheme 6). The Brønsted acid is proposed to act in a bifunctional manner, through a dual hydrogen-bonded transition state with the presumed *ortho*-amino imine intermediate, though the precise interactions of the chiral catalyst backbone with the substrate are not further delineated.



Zhong, Tan, and co-workers have also reported the synthesis of benzimidazoles through a catalyst-controlled Friedel–Crafts amination (Scheme 4).^{4c} Nitrosobenzenes lie at the heart of this strategy, serving both as an electrophilic nitrogen source and oxidant. When a series of *N*-naphthylglycine and *N*-naphthylbenzylamine derivatives **15** were reacted with *ortho*-substituted nitrosobenzenes **16** in the presence of a chiral SPINOL-type CPA **17** or **18**, *N*-arylbenzimidazole products **19** and **20**, respectively, were obtained in up to 97% ee and 84% yield. An interesting stereochemical divergence was observed, where (R_a)-configured CPAs afforded the (R_a) products in the naphthylglycine series, but the (S_a) products for the naphthylbenzylamine derivatives, the latter requiring a copper(II)-based exogenous oxidant. This divergence is attributed to different non-covalent substrate-catalyst interactions. The mechanism proceeds through initial acid-catalysed Friedel–Crafts reaction of the naphthalene with the nitrosobenzene. The resulting *ortho*-diimine undergoes tautomerisation to an amino-imine, followed by enantiodetermining aminal formation, then by oxidation to afford the benzimidazole, with the nitrosoarene evidently a competent oxidant in this step for the glycine-derived series.



Miller and co-workers have also reported the synthesis of a benzimidazole **22** using peptide-based organocatalysts (Scheme 5).¹¹ Cyclo-condensation of phenylenediamine derivative **21** onto an electro-deficient trifluoroacetyl group afforded the axially chiral benzimidazole **22** in 92% ee and 99% conversion in the presence of (R_a)-TRIP **13**, while similar results (88% ee, 99% conversion) were obtained when peptide-based phosphoric acid **23** was used. Use of alternative peptide catalysts **24** and **25** showed that both product enantiomers were accessible by inversion of the *p*Thr phosphoric acid containing amino acid residue alone, demonstrating the versatility of a peptide-based organocatalytic platform. In collaboration with Toste and Sigman, the same laboratory expanded the substrate scope, and further explored the factors influencing enantiocontrol in peptide-based versus BINOL-derived CPAs using DFT and multi-linear regression analysis.¹² While the BINOL-derived CPAs largely operate under steric control due to clashes with the



large 3,3'-aryl groups on the catalyst, the more flexible peptide-based acid was more accommodating of steric bulk in the substrate, highlighting the importance of greater catalyst scaffold diversity in new catalytic applications.

The sole example of catalytic enantioselective cyclocondensation to form a C–N atropisomeric six-membered nitrogen-containing heterocycle was reported by the Tan group in 2017 (Scheme 6).¹⁰ By combining a series of *N*-arylanthranilamides **26** and aromatic and alicyclic aldehydes in the presence of a CPA and DDQ oxidant, the corresponding *N*-arylquinazolinones **27** and **28** were obtained in up to 98% yield and 97% ee. The Brønsted acid is presumed to initially catalyse formation of an imine, then to control stereochemistry in the cyclisation to afford an aminor intermediate, which is oxidised in situ to form the target molecule. Though clearly a powerful approach, the reaction did not proceed satisfactorily for linear aliphatic aldehydes. An alternative C–C bond cleavage approach was devised, where 4-methoxypent-3-en-2-one replaced the aldehyde reactant and undergoes acid-mediated formation of an enaminone, followed by acid-catalysed aminor formation. In this case, a retro-Mannich-type reaction liberates acetone and generates the quinazolinone without the need for an exogenous oxidant. A stronger acid was required, with triflylphosphoramide **30** generating products in up to 97% yield and 96% ee. Control experiments demonstrated that the aminor intermediate undergoes fast C–N bond rotation and is functionally non-atropisomeric. The enantiopurity of the product is therefore suggested to be a consequence of centre-to-axial chirality transfer from the aminor stereogenic centre.

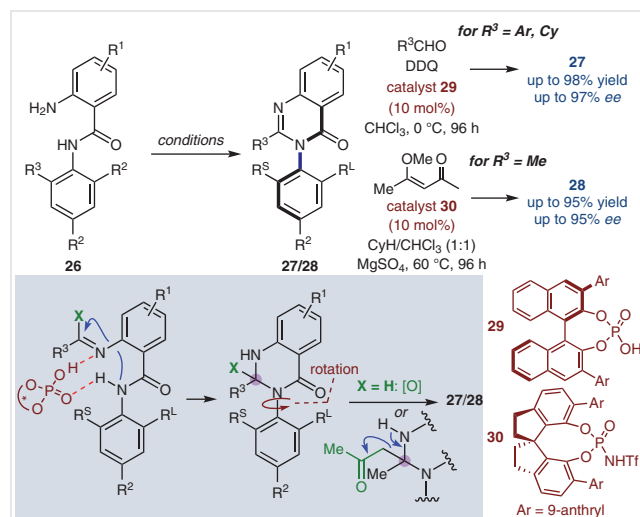
The cyclocondensation route to C–N atropisomers has seen an explosion of interest in recent years. This has largely been enabled by the development of powerful chiral

Brønsted acids, including the peptide-based catalysts introduced by Miller, and by creative strategies such as the use of nitrosobenzenes and the retro-Mannich method used by both Tan and Fu. Through careful study of classical and contemporary condensation approaches to aromatic heterocycles, it is likely that many more enantioselective variants will be uncovered in the years to come.

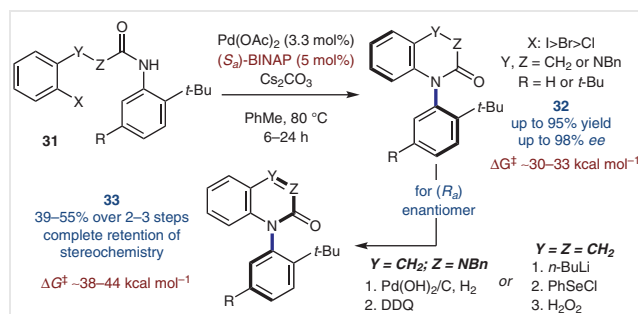
3 Proximal C–N Bond Formation

While the above approach was generally to take classical heterocycle syntheses and render them enantioselective, an alternative strategy is to use the powerful metal-catalysed C–N cross-coupling reactions developed in recent years in the presence of chiral ligands. Steric hindrance hampers atroposelective direct intermolecular axial cross-couplings, but metal-catalysed cyclisation of the pro-axial nitrogen onto a tethered coupling partner is an effective method to generate axial chirality under the directing effect of chiral ligands.

Osamu Kitagawa has been prolific in this approach.^{7d} In 2006 Kitagawa, Taguchi, and co-workers reported a series of inter- and intramolecular *N*-arylations under Buchwald–Hartwig conditions in the presence of chiral phosphine ligands, with (*S_a*)-BINAP proving most effective for the cyclisations, yielding products **32** in up to 95% yield and 98% ee (Scheme 7), with the reaction proceeding in the highest yield with aryl iodide coupling partners **31** (X = I).¹³ While the products were non-biaryl, subsequent studies demonstrated that they could be efficiently oxidised to the corresponding arenes, quinolin-2-ones and quinazolin-2-ones **33**, with no loss of stereochemical integrity.¹⁴ In fact, the oxidised products had significantly higher rotational barriers than the non-aromatic precursors (increases of 6.7–10.4 kcal mol^{−1}), a fact attributed to the ability for the non-aromatic heterocycles to twist in the enantiomerisation transition state, lowering their overall strain energy.

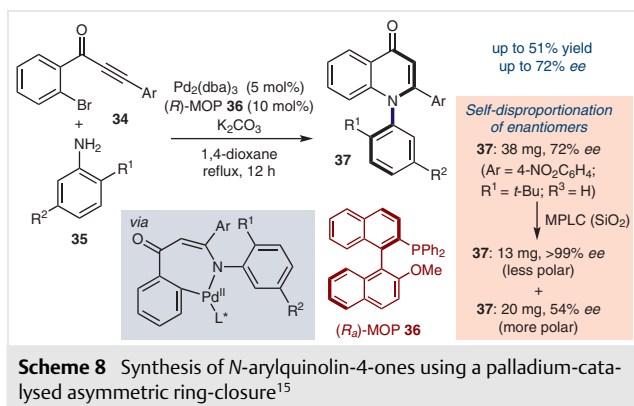


Scheme 6 Brønsted acid catalysed cyclocondensation approach to arylquinazolinones¹⁰



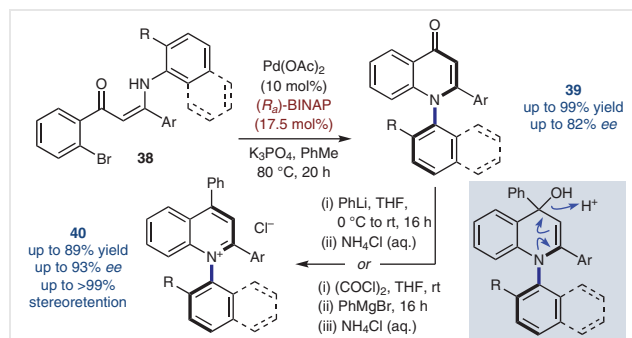
Scheme 7 Atroposelective cyclisation-oxidation approach towards C–N heterobiaryls; Note that the oxidation procedure¹⁴ was conducted on the opposite product enantiomer (formed using (*R_a*)-BINAP) from that obtained in the initial cyclisation report.¹³

In the same year, the Kitagawa group reported the first atroposelective synthesis of quinolin-4-ones using palladium(0) catalysis (Scheme 8).¹⁵ Several *ortho*-substituted anilines **35** were reacted with a series of 2-bromophenyl arylethynyl ketones **34**, producing the corresponding *N*-arylquinolin-4-ones **37** in up to 72% ee and 51% yield under the optimised conditions in the presence of monodentate phosphine ligand (*R_a*)-MOP **36**. The authors note a curious 'self-disproportionation of enantiomers' (SDE) effect under achiral chromatography conditions. When a 72% ee sample was purified by medium-pressure liquid chromatography on silica gel, the less polar, faster-eluting material was found to be enantioenriched (up to >99% ee!), while the later fractions were enantiodepleted (54% ee). This provides a method to obtain highly enantiopure material even in the absence of a highly enantioselective catalytic method, and is further noted in subsequent work from the same laboratory.¹⁶ The reaction proceeds via an initial conjugate addition generating an enaminone intermediate, which undergoes palladium-catalysed ring-closure to afford the *N*-arylquinolin-4-one products.

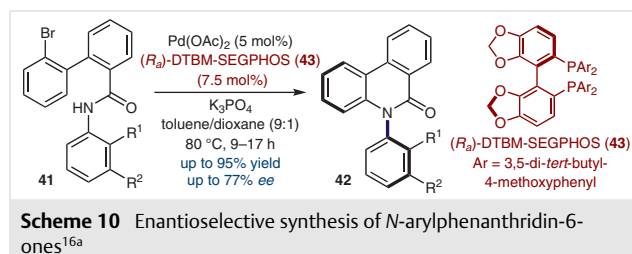


Knipe and co-workers used a similar strategy to afford *N*-arylquinolin-4-ones *en route* to cationic chiral *N*-arylquinolinium salts (Scheme 9).¹⁷ Using as substrates the enaminones **38** presumed as intermediates in the Kitagawa study above, they obtained a series of *N*-(2-*tert*-butylphenyl)- and *N*-naphthylquinolin-4-ones **39** under optimised conditions using Pd(OAc)₂ and (*R_a*)-BINAP in high yields (up to 99%) and variable enantioselectivity (up to 82% ee). A curious enantiodivergence was observed during optimisation: use of (*R_a*)-BINAP led to opposite product enantiomers depending on the palladium source. This was attributed to the in situ reduction of palladium(II) sources by (*R_a*)-BINAP affording (*R_a*)-BINAP(O), a competent ligand that evidently favours the opposite product enantiomer to the parent diphosphine. Organometallic addition into the *N*-arylquinolin-4-ones **39** followed by re-aromatisation afforded *N*-arylquinolinium salts **40** in up to 89% yield and 93% ee, with up to 100% retention of chirality of the parent quinolinone.

The quinolinium salts were shown to exhibit solvatochromatic behaviour, and to possess rotational barriers of 40–51 kcal mol⁻¹.

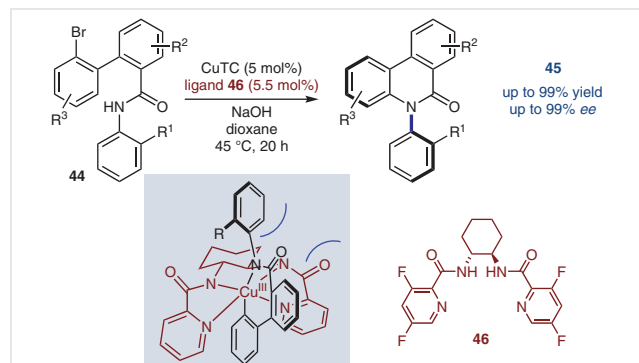


The Kitagawa group further extended the repertoire of palladium-catalysed atroposelective ring-closure to the synthesis of *N*-arylphenanthridin-6-ones (Scheme 10).^{16a} Cyclisation of bromo-anilides **41** with Pd(OAc)₂ in the presence of a chiral bidentate phosphine ligand **43** gave the products in up to 95% yield and 77% ee, with the products displaying the same SDE effect observed previously for *N*-arylquinolin-4-ones.¹⁵



Most intramolecular C–N couplings to form lactam-type biaryl atropisomers operate through palladium-catalysed Buchwald–Hartwig-type reactivity modes, yet some exceptions exist. In 2019, Gu and co-workers reported the first such synthesis using copper-catalysed Ullmann-type coupling (Scheme 11).¹⁸ This approach significantly improved upon the substrate scope and enantioselectivity achieved above under palladium catalysis, suggesting that Ullmann-type couplings may be an under-utilised methodology in atroposelective C–N axis formation. The chiral copper(I) complex formed in situ from copper(I) thiophene-2-carboxylate (CuTC) and a C₂-symmetrical diaminocyclohexane-derived ligand **46** serves as an effective catalyst in the ring closure, affording the products **45** in consistently high yields (up to 99%) and ee (up to 99%). The substrate preference for formation of the *N*-arylphenanthridin-6-one product means additional C–Br bonds can remain unreacted un-

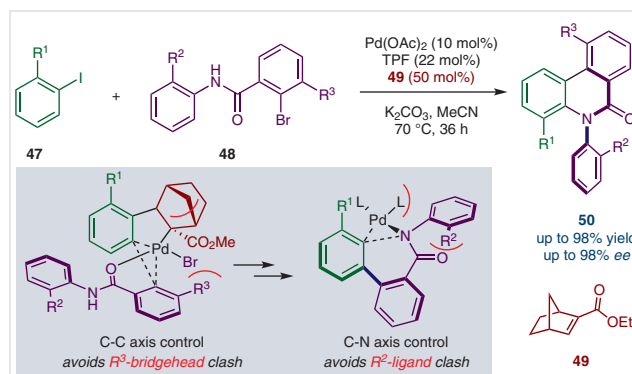
der the optimised conditions, allowing subsequent derivatisation via cross-coupling. The authors propose a Cu(I)/Cu(III) catalytic mechanism where steric clashing between the *ortho*-substituent on the *N*-aryl ring and the ligand picolinamide favours the observed enantiomer.



Scheme 11 Copper-catalysed enantioselective Ullmann-type coupling forming *N*-arylphenanthridin-6-ones¹⁸

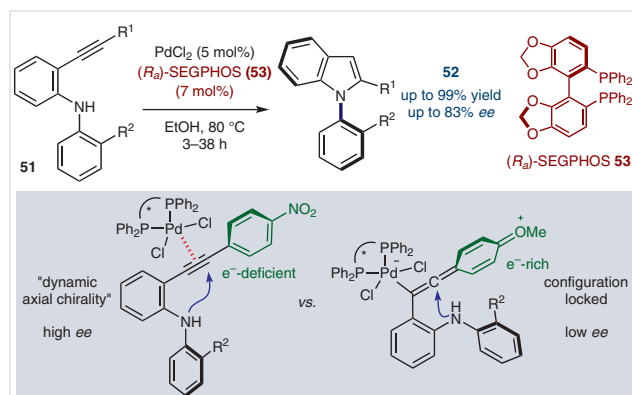
Structurally similar products have also been generated through a palladium-catalysed domino reaction recently reported by Hong, Zhou, and co-workers (Scheme 12).¹⁹ The Catellani reaction between aryl iodides **47** and 2,6-disubstituted aryl bromides **48** catalysed by Pd(OAc)₂, tri(2-furyl)phosphine (TFP), enantiopure norbornene **49**, and potassium carbonate afforded *N*-arylphenanthridin-6-one derivatives **50** in good to excellent yields (up to 98%) and excellent ee (up to 98%). DFT revealed that the reaction occurs via an axis-to-axis chirality transfer mechanism: the initial Catellani-type reaction proceeds through *syn*-carbo-metalation *anti* to the ethylene bridge, followed by C–C bi-aryl axis formation with stereochemistry controlled by the norbornene. This undergoes a subsequent Buchwald–Hartwig-type ring closure under substrate control, where the existing C–C axis controls the C–N axis stereochemistry. The methodology is further extended to the formation of doubly atropisomeric products using diiodobiphenyl and diiodonaphthalene substrates.

Thus far reactions generating amide-type aromatic heterocycles (quinolinones, phenanthridinones etc.) have been discussed. However, metal-catalysed C–N coupling reactions have also provided access to other heterocyclic motifs. In 2010 the Kitagawa group reported the synthesis of C–N atropisomeric indoles by palladium-catalysed intramolecular alkyne hydroamination (Scheme 13).²⁰ Further substrate scope and mechanistic aspects were reported in a subsequent full paper in 2016.²¹ Cyclisation of the 2-alkynylaniline **51** proceeds to form the indole product **52** with up to 99% product yield and 83% ee. A strong dependence on the substrate electronics was observed and quantified by Hammett plot, with electron-rich arenes at the R¹ position giving poor enantioselectivities (R¹ = *p*-MeOC₆H₄: 18% ee) while electron-poor arenes gave much better selectivity (R¹



Scheme 12 Asymmetric Catellani-type reaction towards atropisomeric *N*-arylphenanthridin-6-one and related compounds¹⁹

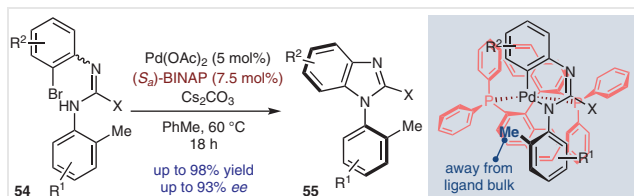
= *p*-O₂NC₆H₄: 79% ee). This observation led the authors to propose a mechanism with the enantiodetermining intermediate existing on a continuum between a η²-alkyne–palladium(II) complex and an allene σ-complex, with the former favoured by electron-poor and the latter by electron-rich substrates. The η²-alkyne complex is said to exhibit ‘dynamic axial chirality’ (since rotation about the alkyne is possible), allowing the ligand to efficiently transfer chirality to the substrate, whilst the allenyl complex is configurationally locked, preventing the relaying of chiral information from the ligand.



Scheme 13 Enantioselective synthesis of *N*-arylindoles via intramolecular alkyne hydroamination²⁰

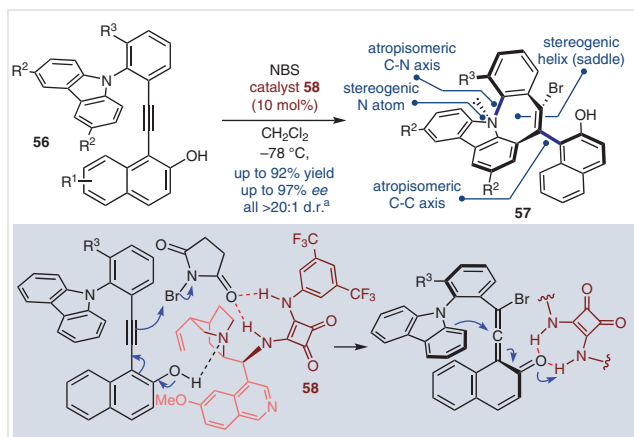
Axially chiral *N*-arylbenzimidazoles have also been formed by proximal C–N cross coupling under palladium catalysis. In 2021 Lu, Liu, and co-workers reported the asymmetric ring-closing Buchwald–Hartwig reaction of a series of amidines (Scheme 14).²² Treatment of the amidines **54** with Pd(OAc)₂ and chiral bidentate ligand (*S_a*)-BINAP gave the *N*-arylbenzimidazole products **55** in up to 98% yield and 93% ee. The method was further extended to the synthesis of dibenzimidazoles from the corresponding diamidines (formed from 1,4-diaminobenzene derivatives), which seemingly benefitted from Horeau amplification giv-

ing products up to 99% ee. The mechanism is presumed to proceed through initial oxidative addition, followed by amidine deprotonation to form the diazaallyl anion, ligand exchange, and reductive elimination. The authors propose a transition state model wherein the diazaallyl palladacycle is positioned in an unhindered quadrant, and the aniline *ortho* substituent is positioned away from the bulk of the ligand structure.



Scheme 14 Buchwald-Hartwig approach to atropisomeric *N*-arylbenzimidazoles²²

In 2021 Yan and co-workers disclosed a remarkable organocatalysed transformation yielding complex azepine skeletons containing a chiral C–N axis, among other stereogenic elements (Scheme 15).²³ Quinine-derived squaramide catalyst **58** induces the substrate **56** to undergo a cascade bromination-cyclisation reaction generating products **57** containing C–C and C–N chiral axes, as well as a stereodefined tertiary amine and a helically chiral saddle-shaped 7-membered ring, proceeding in up to 92% yield and 97% ee and in >20:1 d.r. The authors' mechanistic proposal is that catalyst-controlled bromination generates a chiral bromovinylidene *ortho*-quinone methide intermediate. The stereogenic C–N axis is then forged in the subsequent intramolecular electrophilic aromatic substitution on the prochiral carbazole under substrate control, which is suggested to be the overall rate-determining step. Where the carbazole was unsymmetrical a kinetic resolution was possible, or the reaction could be run to completion with a diastereoselectivity



Scheme 15 Cascade synthesis of chiral azepines. ^a Major/sum of minor diastereomers. R² groups omitted from mechanism for clarity.²³

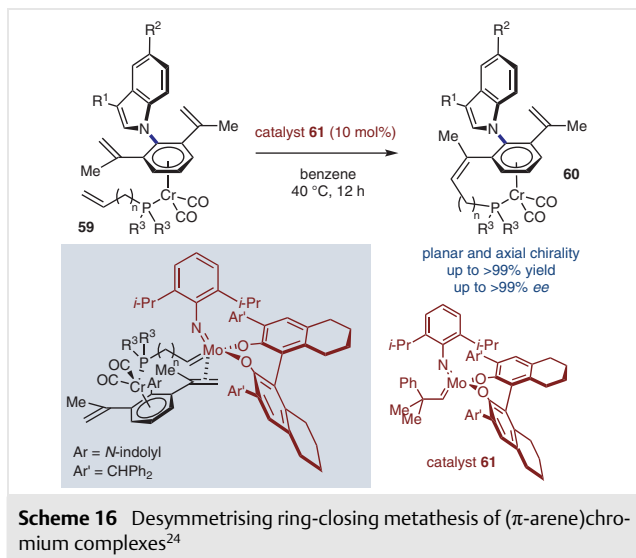
ty of 1.3–1.9:1. Preliminary data suggested that these azepines have potential applications as selective fluorescent sensors for Ru(III).

This final example notwithstanding, the synthesis of C–N atropisomers by intramolecular C–N bond formation is dominated by palladium-catalysed approaches. Despite this there remains little understanding of the catalyst-substrate interactions leading to the observed product atropisomers, and reaction discovery is largely a matter of laborious ligand screening. We hope that physical organic and quantum chemical approaches may be brought to bear on these systems to accelerate reaction development and inspire new ligand and catalyst systems.

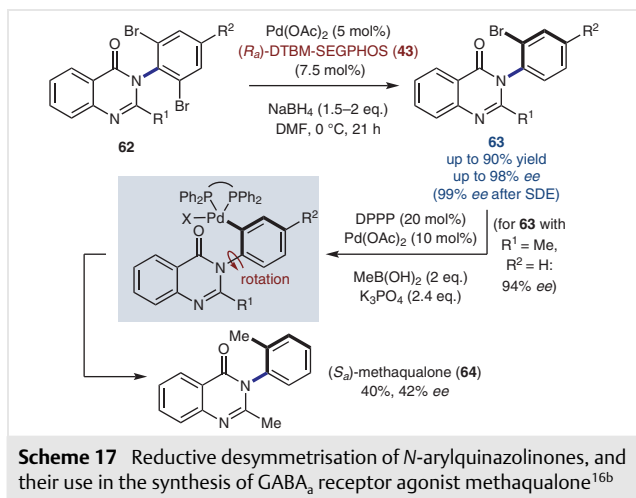
4 Desymmetrisation of Intact Axes

In some substrates, restricted rotation may exist along a C–N axis where a symmetrical substitution pattern means the molecule is achiral. In such instances, desymmetrisation provides a viable route to enantioenriched atropisomeric compounds. In 2015 Kamikawa, Takahashi, Ogasawara, and co-workers reported an interesting double desymmetrisation reaction involving (π -arene)chromium complex **59** through Mo-catalysed asymmetric ring-closing metathesis (Scheme 16).²⁴ A transition state was proposed where after initial metathesis with the less hindered terminal alkene, intramolecular coordination of the metal to the pro-(R_a) alkene favours cyclisation to the observed planar and axial stereoisomer **60**. Since the starting material arylchromium bond is exclusively *anti* relative to the indolyl group and these remain unchanged, the product is obtained as a single diastereomer. Decomplexation of the chromium complexes was achieved in 93–97% yield and with complete retention of stereochemistry upon exposure to sunlight under air in the presence of elemental sulfur.

The Kitagawa group used an asymmetric reductive desymmetrisation approach to access axially chiral *N*-arylquinazolinones (Scheme 17).^{16b} Symmetrical *N*-(2,6-dibromophenyl)quinazolin-4-ones **62** were treated with sodium borohydride in the presence of Pd(OAc)₂ and chiral phosphine ligand **43**, affording a mixture of single **63** and double-reduced (achiral) products. The reaction requires a balance to be struck between yield and enantioselectivity: for example, when a substrate **62** (R¹ = Me; R² = H) was treated with 1.5 equivalents of sodium borohydride the monobrominated product was obtained in 76% yield and 56% ee with just 7% over-reduction; with 2.0 equivalents of reductant the same product was obtained in just 48% yield, but with an increased 73% ee, and 27% over-reduced product. Racemic monobrominated products could also be kinetically resolved, albeit to just 38% ee. The products **63** displayed the self-disproportionation of enantiomers effect discussed previously (Scheme 8). Lastly the monobrominated product was converted into methaqualone (**64**) through

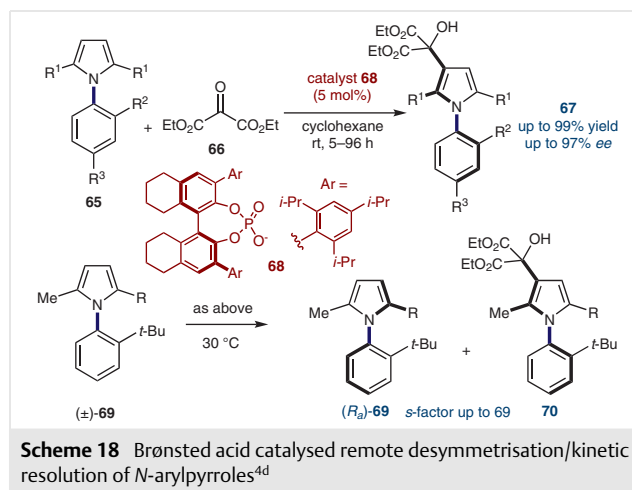


Suzuki cross-coupling, with a 52% loss in ee suggesting a lower barrier to rotation in the intermediate Pd(II) complex. While not discussed by the authors, this may indicate that a *dynamic* kinetic resolution could be achieved in this system if chiral ligands were present on the metal.



C–H functionalisation remote to the C–N axis can also allow access to enantioenriched material, either through desymmetrisation or kinetic resolution. Wang, Tan, and co-workers recently disclosed a Brønsted acid catalysed electrophilic aromatic substitution strategy (Scheme 18):^{4d} treatment of 2,5-disubstituted *N*-arylpyrroles **65** with diethyl oxomalonate (**66**) in the presence of (*S*_a)-H₈-TRIP **68** allowed the desymmetrisation of prochiral substrates in up to 99% yield and 97% ee. Where the existing *ortho*-substituents were non-identical **69** a kinetic resolution gave *s*-factors of up to 69. A mechanism was proposed involving bifurcated hydrogen bonding between the catalyst and elec-

trophile, though the precise reason why this favours reaction with the transient (*R*_a)-atropisomer of the starting material is not discussed. The utility of these compounds was demonstrated: *N*-[*o*-(diphenylphosphino)aryl]pyrrole (*R*² = PPh₂) was a competent ligand for palladium-catalysed asymmetric allylic substitution, giving products in up to 97% ee.

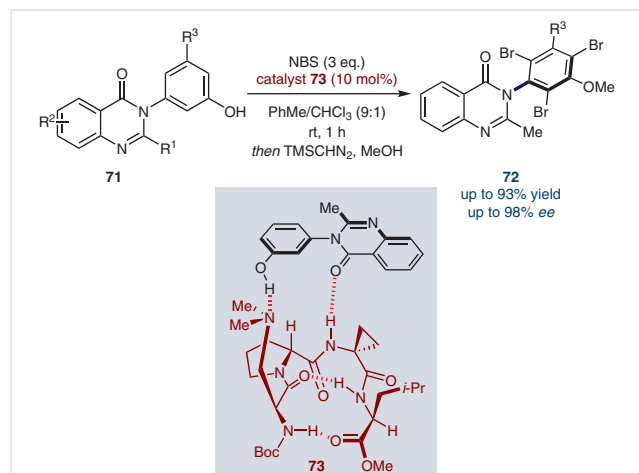


Desymmetrisation can be an elegant approach to C–N atropisomers as shown above, but does place rather stringent requirements on the products that may be obtained since they necessarily must derive from a symmetrical and suitably reactive precursor.

5 *ortho*-C–H Functionalisation

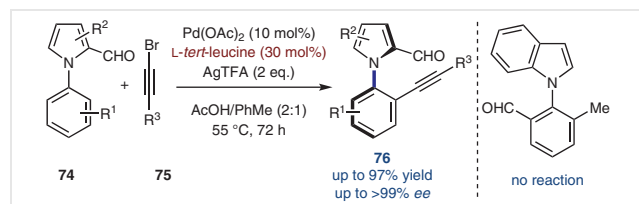
The rapid development of C–H functionalisation strategies in recent years has provided an alternative strategy towards C–N atropisomeric compounds. With the axis already in-place, replacement of an adjacent *ortho*-CH bond with a carbon or heteroatom generally leads to an increase in the rotational barrier. This approach has the potential to be extremely broad due to the ubiquity of such bonds. Miller and co-workers pioneered this strategy for quinazolinones.²⁵ Treatment of the substrate **71** with NBS in the presence of peptide-based organocatalyst **73** afforded tribrominated products **72** in up to 98% ee and 93% yield (Scheme 19). The catalyst is proposed to adopt a type-II' β-turn conformation through X-ray studies. By considering both the catalyst X-ray structure, and solution-phase NOESY experiments, a transition state was proposed invoking dual substrate-catalyst hydrogen bond formation. After the initial bromination the chiral axis is sterically locked, and the subsequent two brominations proceed as expected. Subsequently Miller, Sigman, and co-workers attempted to parameterise and modify the peptide catalyst in an effort to enhance selectivity.²⁶ This study highlighted the impor-

tance of the cyclopropane-containing amino acid, and concluded that although the type-II' β -turn is likely important, the true mechanism involves an ensemble of conformers acting simultaneously.



Scheme 19 Peptide-catalysed bromination of *N*-arylquinazolinones²⁵

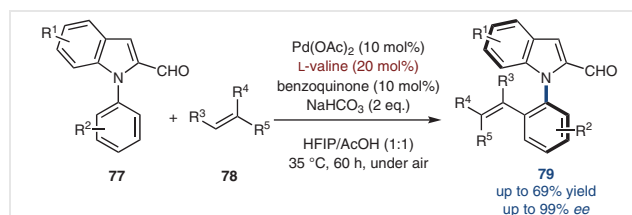
Unsurprisingly, palladium-catalysed C–H functionalisation has also been applied to C–N atropisomeric axes. In 2019 two groups independently reported the atroposelective C–H functionalisation of *N*-aryl-2-formylindoles and pyrroles, with the aldehyde in both cases providing a handle to incorporate a transient imine directing group. Hong, Shi, and co-workers explored a series of pentatomic heteroaromatic biaryls where the aldehyde handle enabled enantioselective C–H alkynylation (Scheme 20).²⁷ When the prochiral aldehyde substrate **74** was reacted with bromoacetylene **75**, catalytic Pd(OAc)₂, and stoichiometric AgTFA, and in the presence of chiral transient director *L*-tert-leucine the pyrrole products **76** were obtained in up to up to 97% yield and >99% ee. The authors were unable to form axially chiral indoles through the same method, with the aldehyde positioned on the benzenoid ring.



Scheme 20 Transient imine-directed C–H alkynylation²⁷

Zhang, Xie, and co-workers circumvented this problem in their palladium-catalysed oxidative Heck reaction by instead positioning the aldehyde on the indole 2-position (Scheme 21).²⁸ When *N*-aryl-2-formylindoles **77** were treated with electron-deficient alkenes (**78**) in the presence of Pd(OAc)₂, *L*-valine, and benzoquinone under air, the cor-

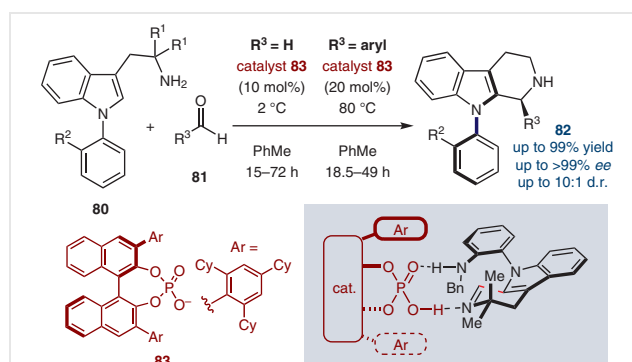
responding oxidative Heck products **79** were formed in good yields and up to 99% ee. Where the benzenoid ring in the starting material bears an *ortho* group the starting materials themselves are axially chiral. By replacing the benzoquinone/air oxidant with AgTFA and increasing the temperature to 60 °C, these compounds underwent kinetic resolution with *s*-factors up to 459.



Scheme 21 Transient imine-directed C–H alkenylation²⁸

Given that both studies above involved similar 2-formyl heterocycles and used *L*-amino acid directing groups, it is unsurprising that the stereochemical outcome in both cases is the same, though neither group proposes a transition state model.

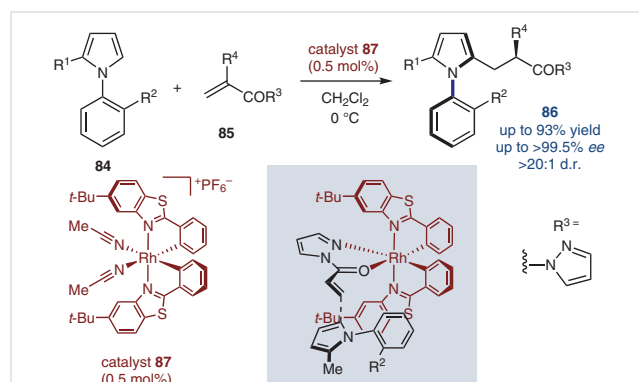
In 2021, Kwon and co-workers disclosed the enantioselective synthesis of *N*-arylindoles via a chiral acid-catalysed Pictet–Spengler reaction (Scheme 22).²⁹ When the substrate **80** is treated with paraformaldehyde in the presence of chiral phosphoric acid **83**, the cyclisation onto the 2-position proceeds smoothly at 2 °C. Electron-deficient aldehydes **81** also reacted, but required an increase in temperature to 80 °C. Electron-neutral and electron-rich aryl aldehydes failed to react. Cyclisation onto the 2-position increases the rotational barrier sufficiently that the products can be obtained in high yield and enantiopurity. R² was typically a hydrogen bond donor such as NHBn, and the importance of this is highlighted in the putative transition state, where this group participates in a hydrogen bond with the catalyst that reduces conformational flexibility. Cyclisation is proposed to proceed via a chair-like transition state to afford the observed major (*S*_a)-stereoisomer. However, assuming the transient imine intermediate is (*E*)-con-



Scheme 22 CPA-catalysed enantioselective Pictet–Spengler reaction²⁹

figured, this does not fully account for the observed diastereochemical outcome in the reaction involving electron-deficient arylaldehydes.

Houk, Meggers, and co-workers disclosed a related strategy using Lewis acid activation (Scheme 23).³⁰ When *N*-arylpyrroles **84** were treated with *N*-(acryloyl)pyrazoles **85** in the presence of Δ -configured chiral Lewis acid **87**, the axial and point chiral products **86** were obtained in up to >99.5% ee, >20:1 d.r. and high yields. Quantum chemical calculations revealed that the (*R_a*)-stereochemical outcome is controlled by a steric clash between *R*² and the *tert*-butyl substituent on the catalyst. The pyrazoles were necessary to achieve the required bidentate binding to the Lewis acid, but were easily removed by reduction to afford the corresponding aldehyde or alcohol, or by substitution to form ester, amide, and cyclic ketone derivatives.



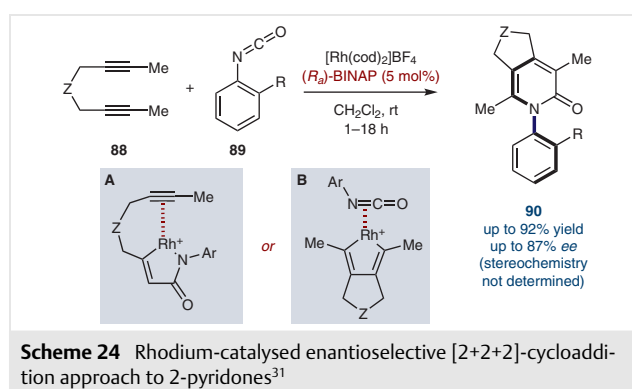
Scheme 23 Lewis acid catalysed synthesis of *N*-aryl pyrroles³⁰

Research into C–H functionalisation in the context of C–N chiral axes remains in its infancy. However, given the growth of C–H functionalisation across synthetic chemistry in recent years, it is likely that this strategy will continue to develop. It is well-suited to this application, since it is almost inevitable that *ortho*-C–H functionalisation will lead to an increase in the rotational barrier around an axis providing a window for dynamic kinetic resolution approaches.

6 Cycloaddition

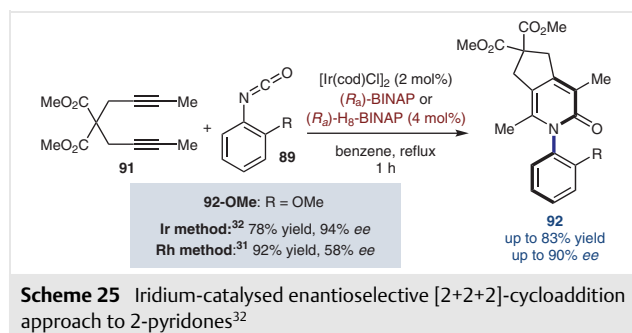
Cycloaddition is an appealing strategy for the formation of C–N atropisomers, allowing the chiral axis to be forged in a convergent manner from simple, achiral precursors. This approach was first explored by Tanaka and co-workers in 2008 (Scheme 24).³¹ They reported the enantioselective synthesis of *N*-aryl-2-pyridones **90** via the rhodium-catalysed formal [2+2+2]-cycloaddition of *ortho*-substituted aryl isocyanates **89** with a series of symmetrical diynes **88**, in the presence of a chiral (*R_a*)-BINAP ligand. Products were

obtained in variable yield and enantiopurity. This variability was rationalised on the basis of two potential reaction pathways, with more-coordinating isocyanates and less-coordinating diynes expected to go via the more stereoselective pathway A, and vice versa for pathway B. The change in the order-of-events renders the presumed stereodetermining step to be either intra- or intermolecular, with the former proposed to give higher enantioselectivities. Though the absolute stereochemistry of products was not determined, we suggest products are (*R_a*) by retrospective comparison of optical rotation data [*R* = OMe, *Z* = C(CO₂Me)] with a literature value.³²



Scheme 24 Rhodium-catalysed enantioselective [2+2+2]-cycloaddition approach to 2-pyridones³¹

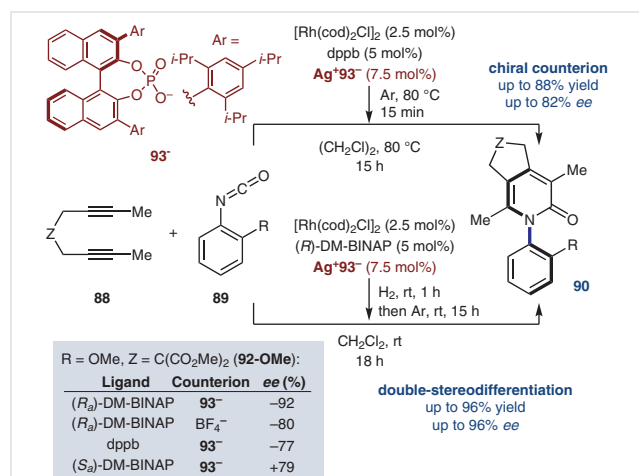
In 2011 Takeuchi and co-workers conducted a wide-ranging study into iridium-catalysed [2+2+2]-cycloadditions.³² They reported an improvement upon the stereoselectivity of the rhodium-catalysed reaction by using an iridium-based catalyst (Scheme 25). Furthermore, the use of reduced ligand (*R_a*)-H₈-BINAP was found to be superior for some substrates, such as methoxy product **92-OMe** (*R* = OMe).



Scheme 25 Iridium-catalysed enantioselective [2+2+2]-cycloaddition approach to 2-pyridones³²

In the rhodium-catalysed study by Tanaka and co-workers³¹ the cationic metal possesses an achiral tetrafluoroborate counterion. Aubert, Fensterbank, Ollivier, and co-workers have explored whether a chiral counterion, both in the presence and absence of a chiral ligand on rhodium, can influence the absolute stereochemistry of the pyridone products. In 2013 they reported that pre-treatment of an achiral

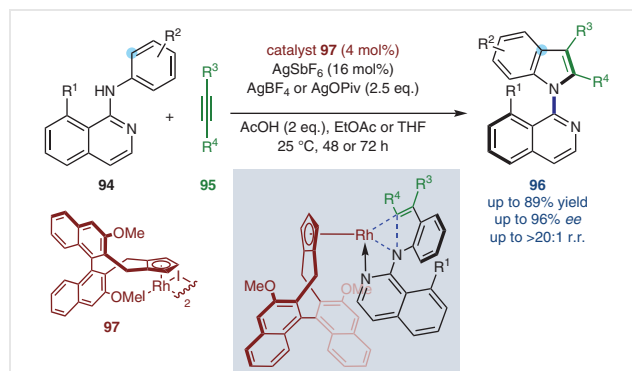
rhodium complex with an (*S_a*)-TRIP-derived chiral silver(I) phosphate afforded a catalytically active ion pair which in many cases out-performed the chiral ligand approach of Tanaka (Scheme 26, top).³³ The 2-pyridone products were obtained in up to 88% yield and 82% ee. In an extension of this study, the case where both the ligand and counterion are homochiral was explored (Scheme 26, bottom).³⁴ After re-optimising the reaction with respect to the chiral ligand, the authors reported evidence of double-stereodifferentiation, where in some cases a matched combination of ligand [(*R_a*)-DM-BINAP] and counterion [(*S_a*)-TRIP-derived phosphate **93⁻] allows product formation in higher ee than in the presence of either chiral species alone. The same product discussed previously **92-OMe** [R = OMe, Z = C(CO₂Me)] was formed in 88% yield and 92% ee under the optimised conditions, but when the chiral ligand alone was present (counterion: BF₄⁻) the ee dropped to 80%, and when the chiral counterion alone was present (ligand: dppb) the ee further fell to 77%. The ligand appears to dominate stereocontrol to a greater extent than the counterion: changing to (*S_a*)-DM-BINAP led to an inversion of the product absolute stereochemistry, albeit with a reduction in ee to 79%.**



Scheme 26 Single and double-stereodifferentiation strategy using chiral phosphate counterions in the synthesis of 2-pyridones via [2+2+2]-cycloaddition^{33,34}

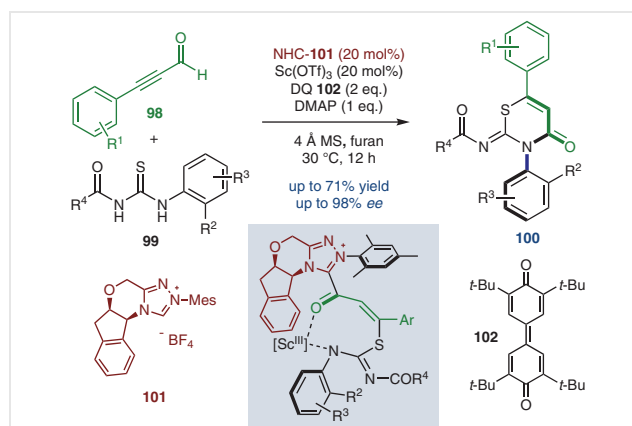
Rhodium catalysis has also been used in formal [3+2]-cycloaddition to generate axially chiral *N*-arylanilines by Wang, Lan, Li, and co-workers (Scheme 27).³⁵ When 1-(arylamino)isoquinoline derivatives **94** were subjected to alkynes **95** in the presence of a chiral rhodium-based catalyst and a silver oxidant, the corresponding *N*-(isoquinolin-1-yl)indole products **96** were obtained in high enantioselectivity (up to 96% ee) and good yields. Where R³ ≠ R⁴ regioisomeric ratios of up to >20:1 were obtained. Kinetic isotope effects indicate that C–H bond breaking is involved in the turnover-limiting step, and based on this and DFT studies the authors tentatively propose a mechanism involving enantiodetermining reductive elimination of a rhodium(III)

species. DFT indicated the atropisomeric outcome of this reductive elimination is controlled by repulsion between the *N*-phenylene group and the methoxy substituents on the binaphthyl ligand.



Scheme 27 [3+2]-Cycloaddition approach to axially chiral *N*-arylanilines³⁵

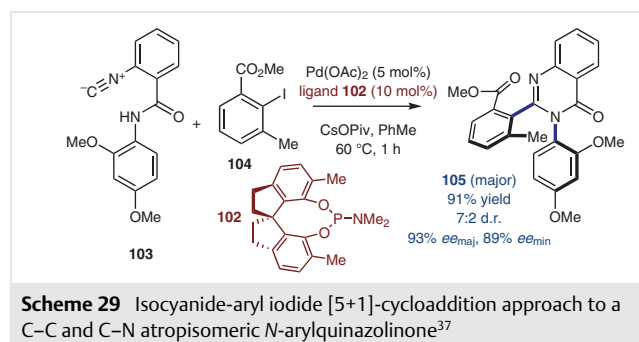
Cycloaddition approaches to C–N biaryl atropisomers are not the sole preserve of group 9 transition-metal-catalysed reactions. In 2021, Jin and co-workers reported the first such synthesis of *N*-arylthiazines catalysed by a chiral *N*-heterocyclic carbene (NHC) organocatalyst (Scheme 28).³⁶ Treatment of a series of ynals **98** with *N*-acyl-*N'*-arylthioureas **99** in the presence of NHC **101**, DMAP, quinone **102**, and Sc(OTf)₃ additive led to a formal [3+3] cycloaddition, with furan the optimal (albeit unusual) solvent. The heterobiaryl *N*-arylthiazine products **100** were obtained in moderate yield (up to 71%) and high enantioselectivity (up to 98% ee). The reaction is proposed to proceed through initial formation of the Breslow intermediate followed by its oxidation to the corresponding alkynyl acylazolium cation, which undergoes conjugate addition with the thiourea. The enantiodetermining step is the subsequent intramolecular *N*-acylation, templated by scandium(III) and with stereo-



Scheme 28 Organocatalysed [3+3]-cycloaddition approach to thiazines³⁶

chemistry controlled by the chiral azolium species, though it is not clear specifically which interactions between R² and the NHC scaffold control the torsional preference about the pro-axial C–N bond.

In a synthetic approach primarily aimed at generating C–C atropisomeric quinazolinones, Luo, Zhu, and co-workers in 2021 reported a palladium-catalysed formal [5+1]-cycloaddition between 2-isocyanobenzamide **103** and aryl iodide **104** coupling partners (Scheme 29).³⁷ In a single example a C–N atropisomeric axis was formed in 91% yield, 7:2 d.r. and 93% and 89% ee of the major and minor diastereomers of the product **105** respectively. Based on mechanistic control experiments the authors propose a reaction sequence involving oxidative addition of palladium into the aryl iodide followed by carbene insertion and cyclisation-reductive elimination to forge the quinazolinone.

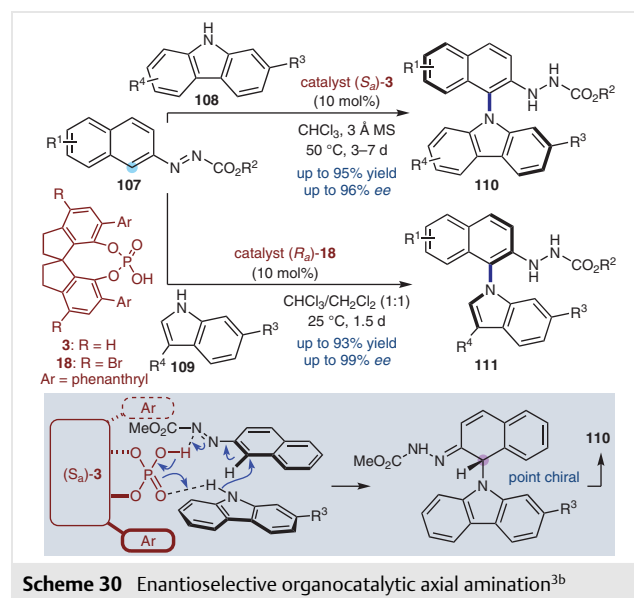


The cycloaddition approach is clearly an expedient method to synthesise axially chiral *N*-aryl-2-pyridones. Prior to 2021 the strategy had not been expanded to encompass any substrate classes beyond those initially reported by Tanaka in 2008. There is clearly a dormant opportunity to exploit this elegant strategy for the synthesis of more diverse C–N atropisomeric scaffolds.

7 Axial C–N Bond Formation

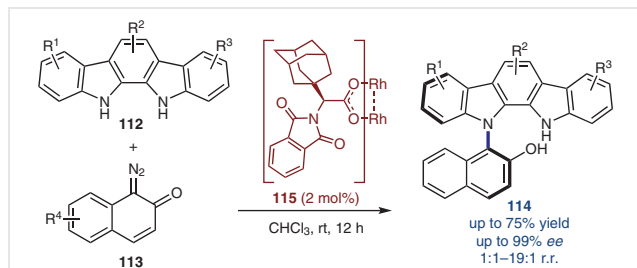
From a retrosynthetic perspective, perhaps the most appealing strategy for the synthesis of C–N atropisomers is direct C–N bond-formation where the bond being formed is the chiral axis itself.³⁸ However, this approach is intrinsically challenging: by their very nature chiral axes are sterically encumbered, and this effect may be even more pronounced for C–N atropisomers than their C–C counterparts due to the shorter bond. For example, there are no reported cases of *intermolecular* atroposelective Buchwald–Hartwig couplings (e.g. of pyridones, quinolones etc.) to form C–N axes. This challenging behaviour may in no small part contribute to the relative success of intramolecular approaches (see Section 3), where the energetic penalty of bringing the reacting partners into close proximity is reduced. Nonetheless, since 2020 several enantioselective axial C–N bond-

forming reactions have emerged. Li, Tan, and co-workers disclosed a LUMO-lowering approach to organocatalytic axial C–N bond formation (Scheme 30).^{3b} A series of azonaphthalenes **107** were treated with carbazoles **108** in the presence of a SPINOL-based chiral phosphoric acid **3**; coordination of the azo group to the acid enhances the electrophilicity of the naphthyl 1-position sufficiently that nucleophilic attack of the carbazole occurs. The atropisomeric products **110** were obtained in up to 96% ee and 95% yield. Indoles **109** were also competent nucleophiles affording products **111** in up to 93% yield and 99% ee with a re-optimised catalyst **18** and protocol. The reaction is proposed to proceed via a dual hydrogen-bonded transition state to a point-chiral intermediate, the stereochemistry of which is efficiently transferred to the chiral axis upon re-aromatisation, though a precise description of the transfer of chirality is not given. The products were converted into phosphine and thiourea derivatives whose potential in asymmetric catalysis applications was demonstrated. Diazonaphthalenes also formed 1,5-dicarbazole naphthalene derivatives containing two chiral axes in up to 98% ee, 57% yield and 4:1 d.r., though a third CPA catalyst was required.



The first metal-catalysed enantioselective axial amination was recently disclosed by Wang and co-workers (Scheme 31).^{3a} Here, the steric repulsion intrinsic to axial C–N bond formation is overcome through the use of a reactive carbenoid intermediate. Diazonaphthoquinones **113** were reacted with indolocarbazoles **112** in the presence of a chiral rhodium-based catalyst **115**, providing *N*-arylcarbazole products **114** in high enantioselectivity and good yield. Where R¹ ≠ R³ regioisomeric ratios varied between 1:1 to 19:1. Upon scale-up, catalyst turnover numbers of 200 were achieved. The authors demonstrated the utility of this method by conducting late-stage functionalisation of natu-

rally occurring and bioactive molecules such as tjipanazole. However, the extremely hindered diazochrysenone failed to react under the optimised conditions, though the racemic reaction [with $\text{Rh}_2(\text{OAc})_4$] did proceed. Lastly, the product phenols were converted into novel chiral phosphoric acids with potential applications in asymmetric organocatalysis.

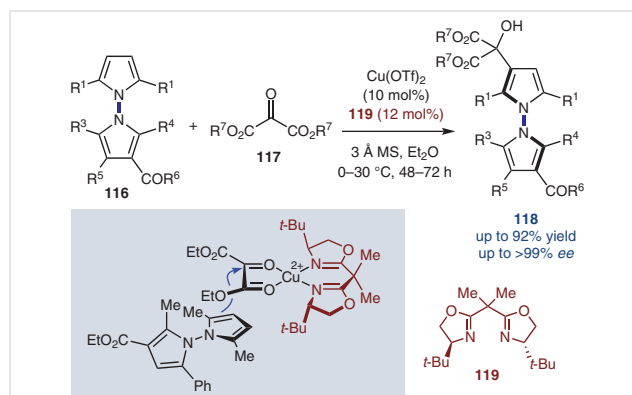


Scheme 31 Rhodium carbenoid approach to axial enantioselective C-N bond formation^{3a}

Despite the elegance and convergency of the approach, direct catalytic axial C-N amination to form atropisomeric heterobiaryls remains in its infancy. However, inspired by these first few reports it seems likely that this approach will see rapid development in the very near future.

8 Atropisomeric N-N Axes: An Emerging Class of Heterobiaryls

The synthesis of atropisomeric molecules possessing N-N chiral axes was, until recently, limited to resolution-based approaches. However, in 2021 Lu, Liu, and co-workers disclosed the first catalytic asymmetric approach (Scheme 32).³⁹ Their strategy resembles that of Wang, Tan, and co-workers (Scheme 18),^{4d} where catalytic activation of an electrophilic oxomalonate enables desymmetrisation of a pre-formed axial bond. Treatment of pre-formed bipyrroles **116** with oxomalonates **117** resulted in alkylation at the 3-position of the more electron-rich and less hindered upper pyrrole (as drawn), and the presence of $\text{Cu}(\text{OTf})_2$ and bisoxazoline ligand **119** led to the products **118** being formed in high yields and enantioselectivities. Kinetic resolution of racemic bipyrroles with *s*-factors up to 173 was demonstrated. Furthermore, other N-N bisazaheterocycles (*N*-naphthyl-, *N*-rhodaninyl-, *N*-quinazolinyl- and *N*-triazinonyl-pyrroles) were reactive under the optimised conditions, though enantioselectivities were generally lower (47–84%) than the bipyrrole series. Stereocontrol was proposed to arise from coordination of the oxomalonate to the square-planar copper(II)-ligand complex. The bipyrrole then proceeds from beneath to avoid steric clash with the *tert*-butyl group, and its approach evidently favours the *pro*-(R_a) atropisomeric conformer.



Scheme 32 Enantioselective synthesis of axial N-N biaryls^{4d}

The importance of chiral hydrazides is not purely esoteric: they have previously been employed as chiral catalysts in their own right.⁴⁰ Whilst this reaction technically falls outside of the scope of this review, it paves the way for future developments in catalytic N-X axial atropisomer synthesis.

9 Conclusion and Outlook

There has been a recent and dramatic explosion in catalytic enantioselective approaches towards biaryl C-N atropisomers: despite reports as early as 2008³¹ over half of the primary literature reviewed was published in the years 2019–2021.⁴¹ This explosion has largely been fuelled by the use of CPAs for cyclo-condensation, but an abundance of other catalytic strategies has emerged. Recently two approaches to the challenging *direct* axial C-N bond formation were disclosed, providing a new, more direct approach to these heterobiaryl atropisomers. A deeper understanding of reaction mechanisms and the origin of asymmetric induction is still needed, so there is an opportunity for physical organic and computational chemists to have a significant impact on this field. A great many C-N heterobiaryl motifs have not yet succumbed to the formation of atropisomeric congeners, but the current pace of development makes further progress a near-certainty.

Conflict of Interest

The authors declare no conflict of interest.

Funding Information

The authors wish to acknowledge financial support from Queen's University Belfast and the EPSRC (SR-EP/R021481/1).

References

- (1) Christie, G. H.; Kenner, J. J. *Chem. Soc., Trans.* **1922**, 121, 614.
- (2) (a) Bock, L. H.; Adams, R. J. *Am. Chem. Soc.* **1931**, 53, 3519. (b) Bock, L. H.; Adams, R. J. *Am. Chem. Soc.* **1931**, 53, 374.
- (3) (a) Ren, Q.; Cao, T.; He, C.; Yang, M.; Liu, H.; Wang, L. *ACS Catal.* **2021**, 11, 6135. (b) Xia, W.; An, Q. J.; Xiang, S. H.; Li, S.; Wang, Y. B.; Tan, B. *Angew. Chem. Int. Ed.* **2020**, 59, 6775.
- (4) (a) Abdellah, I.; Debono, N.; Canac, Y.; Vendier, L.; Chauvin, R. *Chem. Asian J.* **2010**, 5, 1225. (b) Wang, L.; Zhong, J.; Lin, X. *Angew. Chem. Int. Ed.* **2019**, 58, 15824. (c) An, Q. J.; Xia, W.; Ding, W. Y.; Liu, H. H.; Xiang, S. H.; Wang, Y. B.; Zhong, G.; Tan, B. *Angew. Chem. Int. Ed.* **2021**, 60, 24888. (d) Zhang, L.; Xiang, S.-H.; Wang, J. J.; Xiao, J.; Wang, J.-Q.; Tan, B. *Nat. Commun.* **2019**, 10, 566.
- (5) (a) Clayden, J.; Moran, W. J.; Edwards, P. J.; Laplante, S. R. *Angew. Chem. Int. Ed.* **2009**, 48, 6398. (b) LaPlante, S. R.; Fader, L. D.; Fandrick, K. R.; Fandrick, D. R.; Hucke, O.; Kemper, R.; Miller, S. P. F.; Edwards, P. J. *J. Med. Chem.* **2011**, 54, 7005. (c) Toenjes, S. T.; Gustafson, J. L. *Future Med. Chem.* **2018**, 10, 409.
- (6) Skoulidis, F.; Li, B. T.; Dy, G. K.; Price, T. J.; Falchook, G. S.; Wolf, J.; Italiano, A.; Schuler, M.; Borghaei, H.; Barlesi, F.; Kato, T.; Curioni-Fontecedro, A.; Sacher, A.; Spira, A.; Ramalingam, S. S.; Takahashi, T.; Besse, B.; Anderson, A.; Ang, A.; Tran, Q.; Mather, O.; Henary, H.; Ngarmchamnanrith, G.; Friberg, G.; Velcheti, V.; Govindan, R. *N. Engl. J. Med.* **2021**, 384, 2371.
- (7) (a) Bonne, D.; Rodriguez, J. In *Axially Chiral Compounds: Asymmetric Synthesis and Applications*; Tan B., Wiley-VCH: Weinheim, **2021**, 75–108. (b) Cheng, J. K.; Xiang, S. H.; Li, S.; Ye, L.; Tan, B. *Chem. Rev.* **2021**, 121, 4805. (c) Corti, V.; Bertuzzi, G. *Synthesis* **2020**, 52, 2450. (d) Kitagawa, O. *Acc. Chem. Res.* **2021**, 54, 719. (e) Kumarasamy, E.; Raghunathan, R.; Sibi, M. P.; Sivaguru, J. *Chem. Rev.* **2015**, 115, 11239. (f) Li, T.-Z.; Liu, S.-J.; Tan, W.; Shi, F. *Chem. Eur. J.* **2020**, 26, 15779. (g) Takahashi, I.; Suzuki, Y.; Kitagawa, O. *Org. Prep. Proced. Int.* **2014**, 46, 1. (h) Wang, Y.-B.; Tan, B. *Acc. Chem. Res.* **2018**, 51, 534. (i) Zilate, B.; Castrogiovanni, A.; Sparr, C. *ACS Catal.* **2018**, 8, 2981.
- (8) Zhang, L.; Zhang, J.; Ma, J.; Cheng, D.-J.; Tan, B. *J. Am. Chem. Soc.* **2017**, 139, 1714.
- (9) Man, N.; Lou, Z.; Li, Y.; Yang, H.; Zhao, Y.; Fu, H. *Org. Lett.* **2020**, 22, 6382.
- (10) Wang, Y.-B.; Zheng, S.-C.; Hu, Y.-M.; Tan, B. *Nat. Commun.* **2017**, 8, 15489.
- (11) Kwon, Y.; Chinn, A. J.; Kim, B.; Miller, S. J. *Angew. Chem. Int. Ed.* **2018**, 57, 6251.
- (12) Kwon, Y.; Li, J.; Reid, J. P.; Crawford, J. M.; Jacob, R.; Sigman, M. S.; Toste, F. D.; Miller, S. J. *J. Am. Chem. Soc.* **2019**, 141, 6698.
- (13) Kitagawa, O.; Yoshikawa, M.; Tanabe, H.; Morita, T.; Takahashi, M.; Dobashi, Y.; Taguchi, T. *J. Am. Chem. Soc.* **2006**, 128, 12923.
- (14) Suzumura, N.; Kageyama, M.; Kamimura, D.; Inagaki, T.; Dobashi, Y.; Hasegawa, H.; Fukaya, H.; Kitagawa, O. *Tetrahedron Lett.* **2012**, 53, 4332.
- (15) Takahashi, I.; Morita, F.; Kusagaya, S.; Fukaya, H.; Kitagawa, O. *Tetrahedron: Asymmetry* **2012**, 23, 1657.
- (16) (a) Hirata, T.; Takahashi, I.; Suzuki, Y.; Yoshida, H.; Hasegawa, H.; Kitagawa, O. *J. Org. Chem.* **2016**, 81, 318. (b) Hirai, M.; Terada, S.; Yoshida, H.; Ebine, K.; Hirata, T.; Kitagawa, O. *Org. Lett.* **2016**, 18, 5700.
- (17) Sweet, J. S.; Rajkumar, S.; Dingwall, P.; Knipe, P. C. *Eur. J. Org. Chem.* **2021**, 2021, 3980.
- (18) Fan, X. Z.; Zhang, X.; Li, C. Y.; Gu, Z. H. *ACS Catal.* **2019**, 9, 2286.
- (19) Liu, Z.-S.; Xie, P.-P.; Hua, Y.; Wu, C.; Ma, Y.; Chen, J.; Cheng, H.-G.; Hong, X.; Zhou, Q. *Chem* **2021**, 7, 1917.
- (20) Ototake, N.; Morimoto, Y.; Mokuya, A.; Fukaya, H.; Shida, Y.; Kitagawa, O. *Chem. Eur. J.* **2010**, 16, 6752.
- (21) Morimoto, Y.; Shimizu, S.; Mokuya, A.; Ototake, N.; Saito, A.; Kitagawa, O. *Tetrahedron* **2016**, 72, 5221.
- (22) Zhang, P.; Wang, X. M.; Xu, Q.; Guo, C. Q.; Wang, P.; Lu, C. J.; Liu, R. R. *Angew. Chem. Int. Ed.* **2021**, 60, 21718.
- (23) Huang, S.; Wen, H.; Tian, Y.; Wang, P.; Qin, W.; Yan, H. *Angew. Chem. Int. Ed.* **2021**, 60, 21486.
- (24) Kamikawa, K.; Arae, S.; Wu, W.-Y.; Nakamura, C.; Takahashi, T.; Ogasawara, M. *Chem. Eur. J.* **2015**, 21, 4954.
- (25) Diener, M. E.; Metrano, A. J.; Kusano, S.; Miller, S. J. *J. Am. Chem. Soc.* **2015**, 137, 12369.
- (26) Crawford, J. M.; Stone, E. A.; Metrano, A. J.; Miller, S. J.; Sigman, M. S. *J. Am. Chem. Soc.* **2018**, 140, 868.
- (27) Zhang, S.; Yao, Q.-J.; Liao, G.; Li, X.; Li, H.; Chen, H.-M.; Hong, X.; Shi, B.-F. *ACS Catal.* **2019**, 9, 1956.
- (28) Zhang, J.; Xu, Q.; Wu, J.; Fan, J.; Xie, M. *Org. Lett.* **2019**, 21, 6361.
- (29) Kim, A.; Kim, A.; Park, S.; Kim, S.; Jo, H.; Ok, K. M.; Lee, S. K.; Song, J.; Kwon, Y. *Angew. Chem. Int. Ed.* **2021**, 60, 12279.
- (30) Ye, C. X.; Chen, S.; Han, F.; Xie, X.; Ivlev, S.; Houk, K. N.; Meggers, E. *Angew. Chem. Int. Ed.* **2020**, 59, 13552.
- (31) Tanaka, K.; Takahashi, Y.; Suda, T.; Hirano, M. *Synlett* **2008**, 1724.
- (32) Onodera, G.; Suto, M.; Takeuchi, R. *J. Org. Chem.* **2012**, 77, 908.
- (33) Augé, M.; Barbazanges, M.; Tran, A. T.; Simonneau, A.; Elley, P.; Amouri, H.; Aubert, C.; Fensterbank, L.; Gandon, V.; Malacria, M.; Moussa, J.; Ollivier, C. *Chem. Commun.* **2013**, 49, 7833.
- (34) Auge, M.; Feraldi-Xypolia, A.; Barbazanges, M.; Aubert, C.; Fensterbank, L.; Gandon, V.; Kolodziej, E.; Ollivier, C. *Org. Lett.* **2015**, 17, 3754.
- (35) Sun, L.; Chen, H.; Liu, B.; Chang, J.; Kong, L.; Wang, F.; Lan, Y.; Li, X. *Angew. Chem. Int. Ed.* **2021**, 60, 8391.
- (36) Li, T.; Mou, C.; Qi, P.; Peng, X.; Jiang, S.; Hao, G.; Xue, W.; Yang, S.; Hao, L.; Chi, Y. R.; Jin, Z. *Angew. Chem. Int. Ed.* **2021**, 60, 9362.
- (37) Teng, F.; Yu, T.; Peng, Y.; Hu, W.; Hu, H.; He, Y.; Luo, S.; Zhu, Q. *J. Am. Chem. Soc.* **2021**, 143, 2722.
- (38) (a) Frey, J.; Choppin, S.; Colobert, F.; Wencel-Delord, J. *Chimia* **2020**, 74, 883. (b) Thonnissen, V.; Patureau, F. W. *Chem. Eur. J.* **2021**, 27, 7189.
- (39) Wang, X.-M.; Zhang, P.; Xu, Q.; Guo, C.-Q.; Zhang, D.-B.; Lu, C.-J.; Liu, R.-R. *J. Am. Chem. Soc.* **2021**, 143, 15005.
- (40) Mohammadi Ziarani, G.; Fathi Vavsari, V. *Tetrahedron: Asymmetry* **2017**, 28, 203.
- (41) After submission of this review, we reported an additional atroposelective approach to C-N axially chiral N-(2-hydroxyphenyl)pyridones by phase-transfer catalyzed alkylative dynamic kinetic resolution. Sweet, J. S.; Wang, R.; Manesiotis, P.; Dingwall, P.; Knipe, P. C. *Org. Biomol. Chem.* **2022**, DOI: 10.1039/d2ob00177b.